Prediction of Ionospheric Scintillation using Neural Network

Hidayatul Husna Mohd Rozi [1], Mariyam Jamilah Homam [1]*

[1] *Faculty of Electrical and Electronic Engineering,*
   Universiti Tun Hussien Onn Malaysia, Batu Pahat, 86400, MALAYSIA

*Corresponding Author: mariyam@uthm.edu.my

Abstract

Global Navigation Satellite System (GNSS) signals are radio waves that travel through the ionosphere before reaching ground-based receivers. Irregularities in the Earth's ionosphere can make the amplitude and phase of radio signals change rapidly. An understanding of ionospheric scintillations is critical for mitigating positioning errors in GNSS-based applications. The aim of the research is to analyze the ionospheric scintillations over Parit Raja (1°52' N, 103°06' E) from 2017 to 2021, and then to predict the ionospheric scintillations over Parit Raja using neural network. The phase amplitude, $\sigma_\emptyset$ data were collected from a Global Positioning System Ionospheric Scintillation and Total Electron Content Monitor (GISTM) receiver at UTHM. This study used the method of feedforward back propagation neural network to predict of $\sigma_\emptyset$. In this work, data from GISTM receiver from 2017-2021 were analyzed. Results show insignificant phase scintillation between 0.05 rad and 0.1 rad during this period. Various parameters may be utilized to evaluate the precision of the trained model produced by the NN model. Results show that in most set-up of number of neurons in the hidden layer(s), the configuration provides the same RMSE for the training and testing processes. Testing results show predicted values from the neural network are almost the same as the actual values. The error between the actual and predicted values is 4.13% for the phase scintillations. For the future, to facilitate more accurate predictions, the training data set needs to include a greater number of data sets. It is also recommended to combine with other methods such as Genetic Algorithm (GA) and Machine Learning (ML) to get a more accurate prediction.

1. Introduction

Global Navigation Satellite System (GNSS) is a network of satellites that orbit the Earth and provide precise navigation, timing, and positioning. GNSS refers to a broad category of commercial products such as the Global Positioning System (GPS). GNSS signals are radio waves that travel through the ionosphere before reaching ground-based receivers. These signals have a frequency in the order of GHz and therefore interact with small-scale irregularities in the ionosphere (i.e., strong gradients in ion and electron concentrations). This causes the signals to exhibit rapid amplitude and phase fluctuations known as scintillations, leading to position uncertainties and, in severe cases, loss of location [1]. Predicting the effects of space weather is difficult because the interactions between the Sun and the Earth's ionosphere are highly nonlinear. Due to the complexity of the problem, there is no complete theory of ionospheric irregularities and signal scintillation, which limits the predictive capabilities of

physical-based models [2]. The focus of this study is to predict scintillations over Parit Raja (latitude 1°52' N, longitude 103°06' E) by using the neural network method utilizing data from a Global Positioning System Ionospheric Scintillation and Total Electron Content Monitor (GISTM) receiver. Neural networks are composed of small building blocks called neurons that perform a weighted sum of input values to map them to an output value. In the training phase, the neural network "learns" the relation between inputs and targets using known input values that correspond to the predictive attributes which are also known [3]. The analysis of the original data was performed to demonstrate the nonlinearity of the problem.

2. Methodology

2.1 Flowchart of the project

The flowchart in Fig. 1 shows the entire process of implementing this study. The first part of the project is to analyze ionospheric data from 2017 to 2021 using MATLAB. The second part of the project is to predict phase scintillations, $\sigma_\emptyset$ using a Neural Network Toolbox in MATLAB R2021a. The details of each part are described in the following sections.
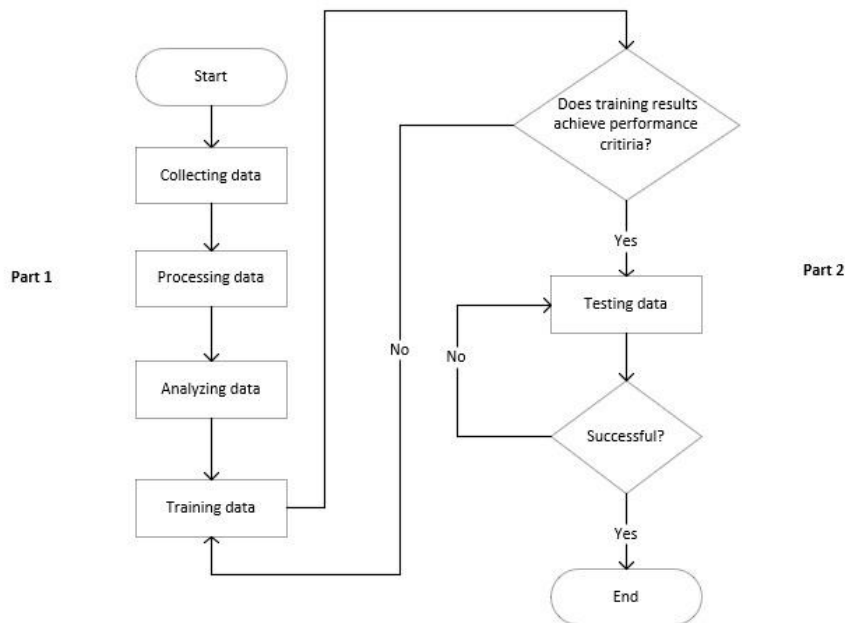
Fig. 1 *Flowchart of the project*

2.2 Part 1: Data analysis

This section provides an explanation of the methods utilized during the analysis of the GISTM receiver's collected data.

2.2.1 Collecting data

The UTHM-installed GISTM receiver is used to collect ionospheric data. The data for amplitude and phase scintillations only covers 2017 to 2021.

2.2.2 Processing data

After processing the raw data from the GISTM receiver, the lock data time for L1 and L2 signals where convergence has not yet occurred has been erased to remove phase scintillations data collected before the phase detrending filter converged. Large phase scintillation data sets are removed to avoid confusion with actual scintillation occurrences. Consequently, any values exceeding 2 rad are discarded. Scintillation amplitudes, typically denoted by the index S4, can be measured by the GISTM receiver. Standardization of the raw amplitude readings is achieved by averaging the readings at 60 second intervals. This produces the total S4, S_{4T} which includes the effects of ambient noise multipath [4]. The calculated trend as shown in equation (2.1). Meanwhile for the $\sigma_\emptyset$, calculate by calculating the standard deviation of the detrended carrier-phase (φ_f) at frequency (f):

$$\sigma_{\varphi f} = \sqrt{\langle \varphi_f{}^2 \rangle - \langle \varphi_f{}^2 \rangle} \qquad (Eq.1)$$

where $\langle \ \rangle$ is the time-windowed expectation over the windows of 1 s, 30 s and 60 s, hence term of phi01, phi30 and phi60, respectively. phi60 is used in this study [5].

2.2.3 Analyzing data

All scintillation data from 2017 to 2021 has been analyzed. The focus of this study is to statistically analyze the characteristics of the ionospheric scintillation observed around Parit Raja, Johor. The overall process of data analysis. Based on the data collection, the influence of solar and geomagnetic field activity on the amplitude and phase scintillation are discussed in depth.

2.3 Part 2: Scintillation prediction

In this part, neural network is used to predict both the amplitude and phase scintillations. Selected sets of data were trained, and then unseen data were tested. Next, the effectiveness of the neural network model was analyzed.

2.3.1 Training data

The method used to train the data in this research is a neural network and the GISTM data used are from 2017 to 2021 to include a wider range of daily SSNs to get more accurate training result. All available data from 2017 to 2021 were used as training data, except data from January, April, July, and October 2021 which were used as testing data. There are five inputs and two targets (i.e. outputs) for the training process.

2.3.2 Testing data

After each iteration of each learning phase, the network is tested for its generalization performance. If the generalization performance is satisfactory, the learning procedure is terminated. The network should be sufficiently trained to learn from the past and predict the future [3]. If only the inputs are presented to the network after it has been trained to learn the relationship between input and output, it can produce the output in the testing phase. The outcomes from the training process were saved, and then applied to the testing process. One month from each season was selected as testing data, which are January, April, July, and October 2021.

3. Results and Discussion

This section discusses the result and analysis of data $\sigma_\emptyset$ from year 2017-2021 and the prediction of ionospheric scintillation using neural network. This project development of the learning application is conducted by using MATLAB for the testing and training data.

3.1 Analysis of ionospheric scintillation

In this study, ionospheric scintillation was analyzed from years 2017-2021 in terms of $\sigma_\emptyset$. These periods correspond to different solar and geomagnetic activity. The daily SSN for January 2017– December 2021 is between 0 and 152, for January, April, July, and October for 2017-2021 the value is between 37 and 103.

3.2 Analysis of phase amplitude

Fig. 2 shows a daily phase scintillation during 2017. The graph shows that the daily value of maximum phase scintillation was in day 315 at 0.079 rad which is considered as very weak scintillation as shown in Table 1. This result was followed by day 324 at 0.072rad. Meanwhile, the minimum value of the daily phase scintillation in 2017 was 0.054 rad on day 347. Fig. 2 to Fig. 6 show the daily phase scintillations for 2018, 2019, 2020 and 2021, respectively. Observation for other years (2018-2021) revealed that daily phase scintillation during this period is very weak. The minimum and maximum daily $\sigma_\emptyset$ for each year is shown in Table 2.

Table 1 *Case consideration for phase scintillation*

Case	$\sigma_\emptyset \ (rad)$
Strong	$0.5 < \sigma_\emptyset \leq 0.6$
Moderate	$0.25 < \sigma_\emptyset \leq 0.5$
Weak	$0.1 < \sigma_\emptyset \leq 0.25$
Very Weak	$0.05 < \sigma_\emptyset \leq 0.1$
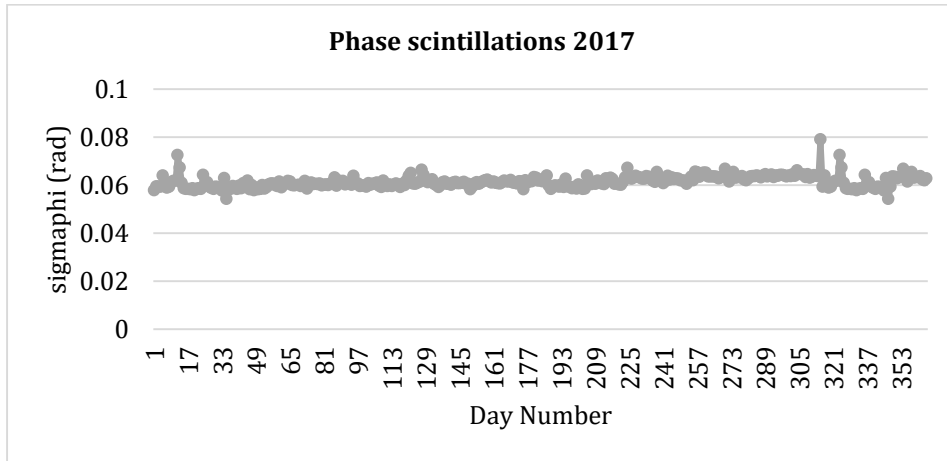
Fig. 2 *Phase scintillations daily value of 2017*
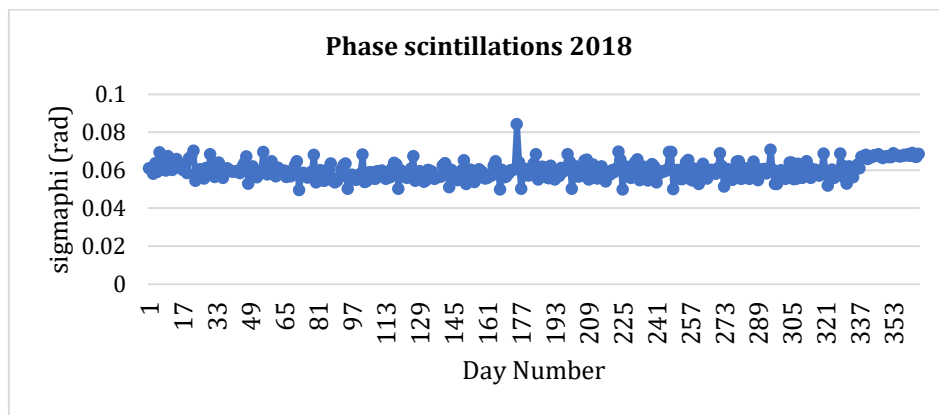
Fig. 3 *Phase scintillations daily value of 2018*
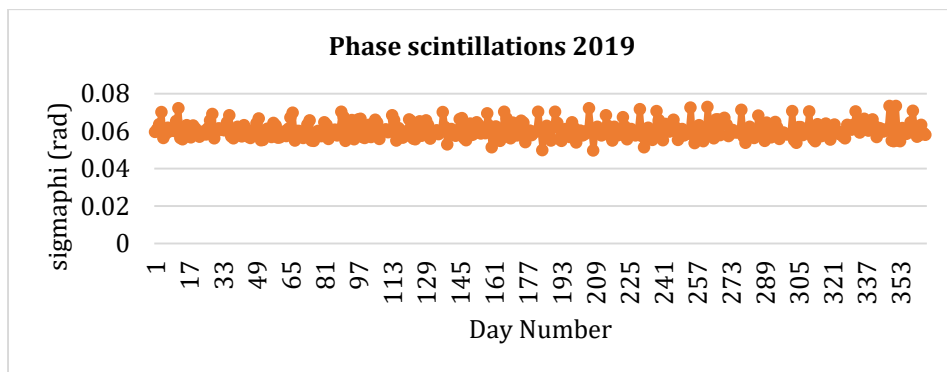
Fig. 4 *Phase scintillations daily value of 2019*
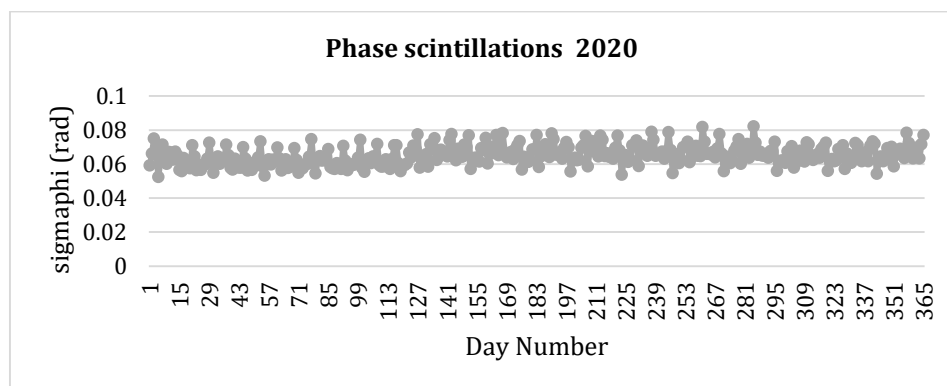
Fig. 5 *Phase scintillations daily value of 2020*
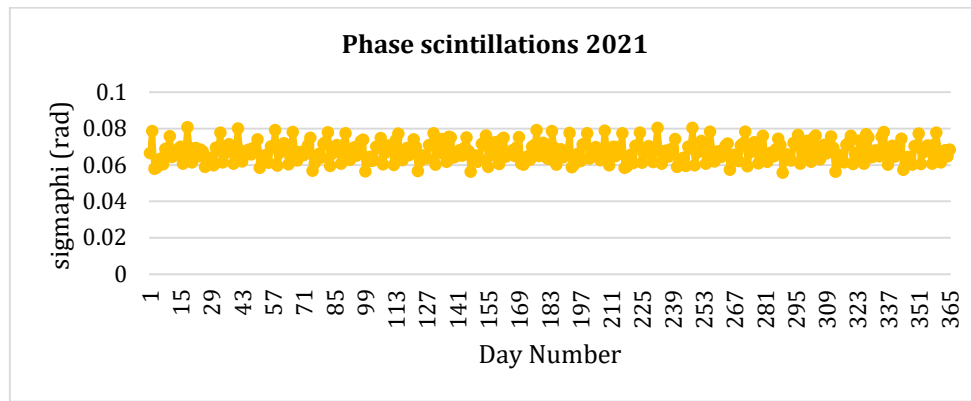
Fig. 6 *Phase scintillations daily value of 2021*

Table 2 *Minimum and maximum daily value of phase*

Year	Maximum daily $\sigma_\emptyset$	Minimum daily $\sigma_\emptyset$
2017	0.054	0.079
2018	0.049	0.084
2019	0.049	0.073
2020	0.052	0.082
2021	0.055	0.081

3.3 Training results

The training process has been completed effectively. All trained networks' parameters were saved and afterwards applied to the testing procedure. Table 3 illustrates the RMSE for a procedure in which the training set consisted of all data from 2017 to 2021 (daily SSN 0- 152) and the testing set consisted of January, April, July, and October data from 2021 (daily SSN 37-103). There are five inputs consisting of 1429 datasets and two targets consisting of 1429 datasets for the training process. The inputs for the neural network have been considered from the parameters known to affect the $\sigma_\emptyset$.

Table 3 *RMSE results for different number of hidden neurons*

No. of neurons in hidden layer	Training	Testing
10	7.28×10^{-4}	1.23×10^{-3}
20	7.28×10^{-4}	1.23×10^{-3}
30	7.74×10^{-4}	8.08×10^{-3}
40	7.79×10^{-4}	1.43×10^{-3}
50	6.75×10^{-4}	1.65×10^{-3}

Results show that in most set-up of number of neurons in the hidden layer(s), the configuration provides the same RMSE for the training and testing process. Overall, the results in Table 3 were better than RMSE because of the smaller number. There is no pattern in the number of neurons chosen for the hidden layer(s) or the number of hidden layer(s). More than one hidden layer hasn't always improved the neural network's ability to predict outcomes accurately. On the other hand, it could improve the training process. According to the findings, training with a larger number of neurons required more time and did not improve the RMSE. With all the neuron numbers 10, 20, 30, 40 and 50 in the configuration above, all resulted for the training RMSE from 6.75×10^{-4} to 7.79×10^{-4} meanwhile the results of the testing RMSE from 1.23×10^{-3} to 8.08×10^{-3} has been observed in Parit Raja stations and it can be higher depending on the time of the solar conditions. From all these configurations all the setup of the neuron numbers has given the same RMSE. However, in this case hidden neuron number 10 has been chosen because the smaller neuron number takes less time for the training process

3.4 Testing result

To evaluate the performance of the NN, only 6.67% of the whole data set was utilized in the testing phase. Because of the phenomena associated with all three seasons, namely the summer solstice, the winter solstice, and the

equinox, the procedure of testing required data from the months of January, April, July, and October 2021. The range of SSN and Kp index for these four months are represented in Table 4.

Table 4 *Range of SSN and Kp index for four months of testing*

Months	SSN	Kp index
January	11.4-12.6	0-3⁺
April	16.0-17.6	0-5
July	20.1-22.7	0-2⁺
October	22.8-32.5	0-5

3.5 Prediction of phase scintillation

The next phase involves implementing the NN model to make predictions for the values $\sigma_\emptyset$ and a modeling period of four months. To accomplish this goal, the physical parameters that are associated with the ionospheric abnormalities that were discussed in the preceding sections are utilized as input data for the forecast day. After that, $\sigma_\emptyset$ forecasted for the period that was specified using the trained by NN. The predicted data for the four months are presented in Table 4. The values for the $\sigma_\emptyset$ the parameter in January, April, July, and October are the same as those in the previous parameter, S4. According to the data presented in Table 5 scintillation of $\sigma_\emptyset$ is more likely to be seen in January because when taking into consideration the less error percentage of 4.13% and the regression of the testing 0.60 which is good because close to the 1. The ionospheric scintillations are plotted against the day number, with both the actual and predicted $\sigma_\emptyset$ data values shown in Fig. 7.

Table 5 *The phase scintillation prediction testing result using the NN model during 30 days in January, April, July and October of 2021*

	2021			
Period	1-31 January	1-30 April	1-31 July	1-31 October
RMSE	1.23×10^{-3}	1.23×10^{-3}	1.23×10^{-3}	1.23×10^{-3}
Regression, R	0.60	0.50	0.60	0.50
Average Error (%)	4.20%	3.24%	4.96%	4.32%
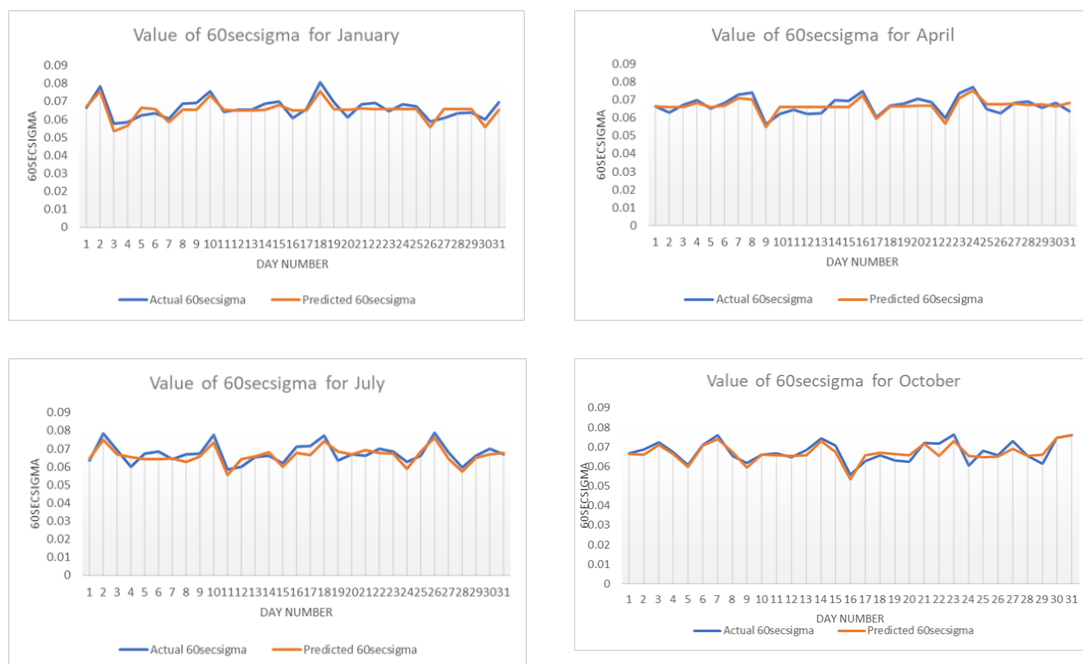
Fig. 7 *Predicted and actual values of $\boldsymbol{\sigma_\emptyset}$ for January, April, July, and October 2021*

4. Conclusion

An investigation of the ionospheric scintillations at Parit Raja, Johor, was being done. To complete this study objective has been done successfully which are the data from GISTM receiver from 2017-2021 were analyzed. Meanwhile, for the training process the parameters of this investigation, five separate types of ionosphere physical data were used as input and two $\sigma_\emptyset$ output information for the NN. This information was then utilized to estimate and forecast the value of for January, April, July, and October 2021. This study focused on the ability of a neural network to make value predictions throughout periods of low to high solar activity using data collected from GISTM receiver from 2017 to 2021. According to the findings, the neural network has the potential to be an effective method for making predictions regarding $\sigma_\emptyset$ values. In some setups of the network, an RMSE and regression that were deemed acceptable were reached. The overall testing produced an RMSE that ranged from 1.23×10^{-3} to 8.08×10^{-3}, an average error that was between 91% and 93%, and a regression coefficient that was between 0.50 and 0.60.

Acknowledgement

Conflict of Interest

Authors declare that there is no conflict of interests regarding the completing of the paper.

Author Contribution

The author attests to having sole responsibility for the following: planning and designing the study, data collection, analysis and interpretation of the outcomes, and paper writing.

References

[1] De Paula, E.; Rodrigues, F.; Iyer, K.; Kantor, I.; Abdu, M.; Kintner, P.; Ledvina, B.; Kil, H. Equatorial anomaly effects on GPS scintillations in brazil. Adv. Space Res. 2003, 31, 749–754.

[2] Kara Lamb, Garima Malhotra, Athanasios Vlontzos, Edward Wagstaff, Atılım Günes Baydin, Anahita Bhiwandiwalla, Yarin Gal, Alfredo Kalaitzis, Anthony Reina, Asti Bhatt. (2019). Prediction of GNSS Phase Scintillations: A Machine Learning Approach.

[3] Haykin, S. 2009. Neural Networks and Learning Machines.3rded. Pearson Education Inc.

[4] GSV GPS Silicon Valley, GSV4004B GPS Ionospheric Scintillation & TEC Monitor (GISTM) User's Manual, 2007.

[5] Van Dierendonck, A.; Arbesser-Rastburg, B. Measuring Ionospheric Scintillation in the Equatorial Region over Africa, Including Measurements from SBAS Geostationary Satellite Signals. In Proceeding of the ION GNSS 17th Technical Meeting of the Satellite Division, Long Beach, CA, USA, 21–24 September 2004